

# Isospin effects on two-particle correlation functions in $E/A = 61$ MeV $^{36}\text{Ar} + ^{112,124}\text{Sn}$ reactions

R. Ghetti<sup>1</sup>, V. Avdeichikov, B. Jakobsson, P. Golubev

*Department of Physics, Lund University, Box 118, S-22100 Lund, Sweden*

J. Helgesson

*School of Technology and Society, Malmö University, S-205 06 Malmö, Sweden*

N. Colonna, G. Tagliente

*INFN and Dip. di Fisica, V. Amendola 173, I-70126 Bari, Italy*

H.W. Wilschut, S. Kopecky, V.L. Kravchuk

*Kernfysisch Versneller Instituut, Zernikelaan 25 NL 9747 AA Groningen, The Netherlands*

E.W. Anderson, P. Nadel-Turonski, L. Westerberg

*The Svedberg Laboratory, Box 533, S-75121 Uppsala, Sweden*

V. Bellini, M.L. Sperduto, C. Sutura

*Laboratori Nazionali del Sud (INFN), Via S. Sofia 44, I-95123 Catania, Italy*

Small-angle, two-particle correlation functions have been measured for  $^{36}\text{Ar} + ^{112,124}\text{Sn}$  collisions at  $E/A = 61$  MeV. Total momentum gated neutron-proton ( $np$ ) and proton-proton ( $pp$ ) correlations are stronger for the  $^{124}\text{Sn}$ -target. Some of the correlation functions for particle pairs involving deuterons or tritons ( $nd$ ,  $pt$ , and  $nt$ ) also show a dependence on the isospin of the emitting source.

PACS number(s): 25.70.Pq

<sup>1</sup>Corresponding Author: Roberta Ghetti, Department of Physics, Lund University, Sweden *E-mail address:* roberta.ghetti@nuclear.lu.se

The isospin dependence of the nuclear equation of state (EOS) is probably the most uncertain property of neutron-rich matter. This property is essential for the understanding of extremely asymmetric nuclei and nuclear matter as it may occur in the  $r$ -process of nucleosynthesis or in neutron stars [1]. In order to study the isospin-dependent EOS, heavy ion collisions with isotope separated beam and/or target nuclei can be utilized [2]. In these collisions, excited systems are created with varying degree of proton-neutron asymmetry. A noticeable isospin dependence of the decay mechanism has been predicted [3–7]. Sensitive observables should be: pre-equilibrium neutron/proton emission ratio [8], isospin “fractionation” [9–12], isoscaling in multifragmentation [13], neutron and proton flows [14].

Recently, the two-nucleon correlation function has been considered as a probe for the density dependence of the nuclear symmetry energy [15,16]. In this theoretical study with an isospin-dependent transport model (IBUU), it was shown that a stiff EOS causes high momentum neutrons and protons to be emitted almost simultaneously, thereby leading to strong correlations. A soft EOS delays proton emission, which weakens the  $np$  correlation. In this paper we study experimental two-particle correlation functions of systems similar in size, but with different isospin. This work shows that, indeed, an isospin signal can be derived.

Two-particle correlation functions were measured in  $E/A = 61$  MeV  $^{36}\text{Ar}$ -induced collisions on isotope-separated targets of  $^{112}\text{Sn}$  and  $^{124}\text{Sn}$ . The experiment was performed at the AGOR Superconducting Cyclotron of KVI (Groningen). The interferometer consisted of 16 CsI(Tl) detectors for light charged particles, mounted at a distance 56–66 cm from the target in the angular range  $30^\circ \leq \theta \leq 114^\circ$ , and 32 liquid scintillator neutron detectors, mounted 2.7 m from the target behind the “holes” of the CsI array, in matching positions to provide the  $np$  interferometer [17]. In this analysis, only data from the angular range  $60^\circ \leq \theta \leq 120^\circ$  were used for neutrons. Finally, 32 phoswich modules from the KVI Forward-Wall were mounted in the angular range  $6^\circ \leq \theta \leq 18^\circ$ , to collect information on the centrality of the collision. At least one fragment in the Forward-Wall was always required in our selected events, which biases our data towards mid-peripheral collisions [18,19]. Energy thresholds for  $p$ ,  $d$ ,  $t$  in the CsI(Tl) detectors were 8, 11, 14 MeV respectively, and for neutrons in the liquid scintillators 2.0 MeV. Details about the experimental setup and the particle energy determination are given in Refs. [17,19,20].

Fig. 1 shows the ratios of the  $n$ ,  $p$ ,  $d$  and  $t$  kinetic energy yields measured in  $^{36}\text{Ar} + ^{124}\text{Sn}$  and  $^{36}\text{Ar} + ^{112}\text{Sn}$  (note the different scale in the figure for  $n$  as compared to  $p$ ,  $d$  and  $t$ ). An equal number of events is sorted for the two Sn-targets. The different solid angle coverage of  $n$  and  $p$  detectors is accounted for, and the neutron energy is efficiency corrected [17]. One can notice not only a substantial enhancement of the  $n$  yield for the neutron-rich system (as may be expected), but also that the enhancement is strongly energy dependent. Furthermore, the  $p$  yield is reduced at low energies for the neutron-rich system, and the  $t$  yield is enhanced over the whole energy range. On the other hand, the yields of the deuteron spectra are the same for the two systems.

The correlation function,  $C(\vec{q}, \vec{P}_{tot}) = k N_c(\vec{q}, \vec{P}_{tot}) / N_{nc}(\vec{q}, \vec{P}_{tot})$ , is constructed by dividing the coincidence yield ( $N_c$ ) by the yield of uncorrelated events ( $N_{nc}$ ) constructed from the product of the *singles* distributions [18].

$\vec{q} = \mu(\vec{p}_1/m_1 - \vec{p}_2/m_2)$ , where  $\mu$  is the reduced mass, is the relative momentum, and  $\vec{P}_{tot} = \vec{p}_1 + \vec{p}_2$  is the total momentum of the particle pair. The correlation function is normalized to unity at large values of  $q$ ,  $80 < q < 120$  MeV/c for  $pp$  and  $np$ , and  $160 < q < 200$  MeV/c for all other particle pairs.

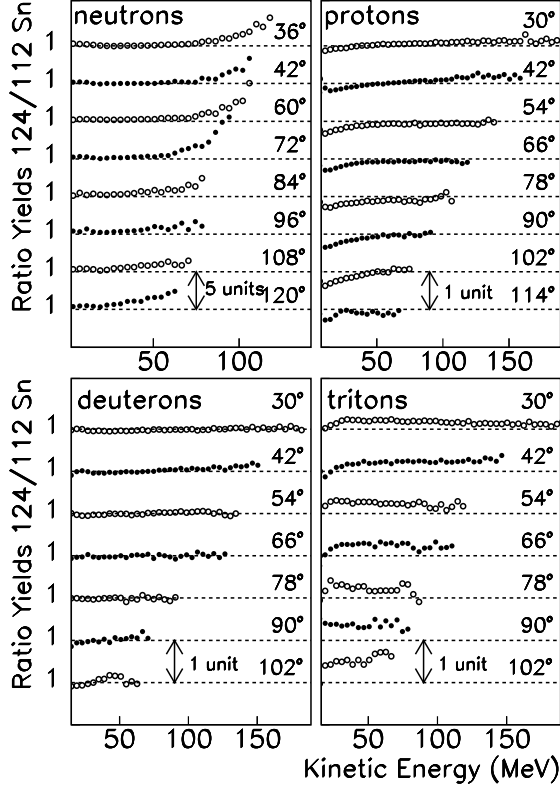


FIG. 1. Ratios of the  $n$ ,  $p$ ,  $d$  and  $t$  kinetic energy yields measured in  $^{36}\text{Ar}+^{124}\text{Sn}$  and  $^{36}\text{Ar}+^{112}\text{Sn}$ . The ratios are arbitrarily shifted in the y-axis (by 5 units for  $n$ , by one unit for  $p$ ,  $d$ ,  $t$ ). The dashed lines correspond to unitary ratios (at the angles indicated in the figure).

The  $54^\circ \leq \theta \leq 114/120^\circ$   $pp/np$  correlation functions are presented in Figs. 2a,b. The neutron energy threshold is here 8 MeV, to match the proton threshold. The shape of the correlation functions looks as expected from the interplay of quantum statistical and final state interactions. Comparing the two Sn-targets, one observes a small but hardly significant enhancement of the correlation strength for  $^{124}\text{Sn}$ , in both  $pp$  and  $np$  correlation functions. For the interpretation of the correlation data, it is important to note that the correlation function depends on the space-time extent of the emitting source. From the size of the source, a stronger correlation is expected for the smaller  $^{36}\text{Ar}+^{112}\text{Sn}$  system, an effect expected also because of the larger excitation energy per particle available for this system (yielding a shorter emission time). On the other hand, the change in neutron number implies a different symmetry energy which also

affects the  $n$  (and  $p$ ) emission times. Neutrons are expected to be emitted faster in the neutron-rich system, which would lead to an enhancement of the correlation strength for  $^{36}\text{Ar}+^{124}\text{Sn}$ . Thus, the net influence on the correlation function is not easily predictable, both due to the uncertainty in the symmetry energy and to the presence of more than one source of emission.

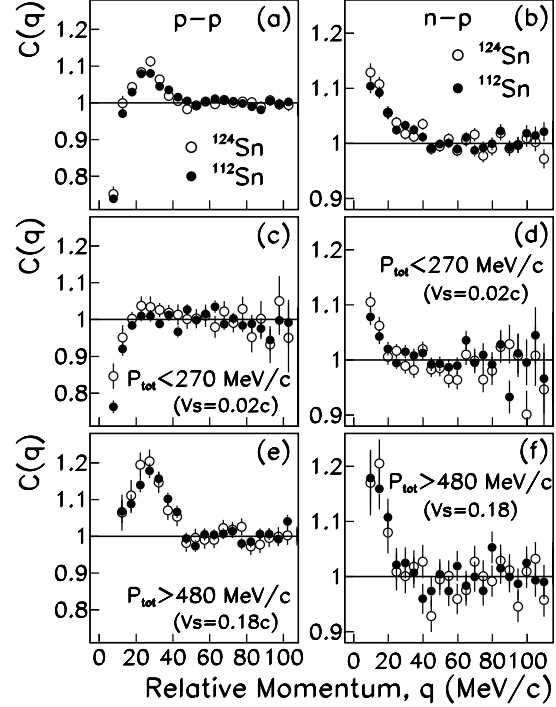


FIG. 2. Angle-integrated ( $54^\circ \leq \theta \leq 114/120^\circ$ )  $pp$  (a,c,e) and  $np$  (b,d,f) correlation functions from  $^{36}\text{Ar}+^{112}\text{Sn}$  (filled circles) and  $^{36}\text{Ar}+^{124}\text{Sn}$  (open circles). Low- $P_{tot}$  (c,d) and high- $P_{tot}$  gated (e,f) correlation functions are also shown.

The emission of light particles from 61 A MeV (mid-peripheral) heavy ion reactions originates from (at least) three sources, a projectile-like (PLS) and a target-like (TLS) evaporative sources (statistical evaporation, SE) and an intermediate velocity source (IS). The IS source represents dynamical emission (DE), which is described either by early nucleon-nucleon collisions or by other pre-equilibrium processes. Some evidence for the creation of a “neck-source” with low density [21–29] has recently been presented, and this may well comprise the dominating part of the DE source. By selecting nucleon pairs with high (low) total momentum, in the proper emission source frame, the DE (SE) emission should be favored. In the following, the  $P_{tot}$  distributions for  $pp$  and  $np$  pairs are calculated in the frame of forward moving sources of velocity  $0.02c$  (TLS) or  $0.18c$  (IS). These velocities are estimated from Maxwell-Boltzmann fits to the singles energy distributions. Low- and high- $P_{tot}$  selections correspond to 20–35% of the total correlation yields.

Figs. 2c,d present the  $pp$  and  $np$  correlation functions

gated on low- $P_{tot}$ . The  $pp$  correlation function is sensitive to this gate, and a suppression in the correlation strength is observed, while the  $np$  correlation function is only slightly suppressed. This is a first hint that the  $np$  correlation function may be dominated by DE.

Figs. 2e,f present the  $pp$  and  $np$  correlation functions gated on high- $P_{tot}$ . Both  $pp$  and  $np$  correlation functions are affected and, in accordance with earlier observations [18], an enhancement in the correlation strength is observed relative to the ungated correlation functions.

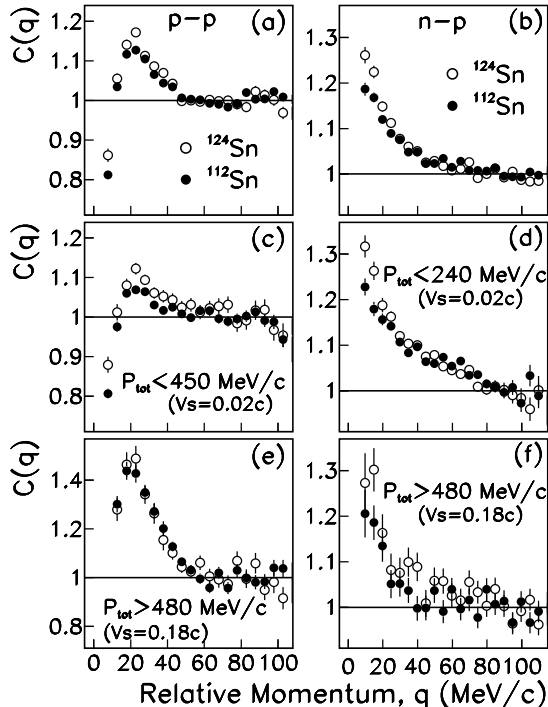


FIG. 3.  $pp$  correlation functions (a,c,e) measured in the forward detectors  $30^\circ \leq \theta \leq 42^\circ$ , and  $np$  correlation functions (b,d,f) measured in the range  $54^\circ \leq \theta \leq 120^\circ$ , with  $E_n \geq 2$  MeV and  $E_p \geq 8$  MeV, from  $^{36}\text{Ar}+^{112}\text{Sn}$  (filled circles) and  $^{36}\text{Ar}+^{124}\text{Sn}$  (open circles). Low- $P_{tot}$  (c,d) and high- $P_{tot}$  gated (e,f) correlation functions are also shown.

All results from these angle integrated data ( $54^\circ$ – $114/120^\circ$ ) show smaller isospin effects than could be expected from the  $N/Z$  ratio, which is 1.18 for  $^{36}\text{Ar}+^{112}\text{Sn}$  and 1.35 for  $^{36}\text{Ar}+^{124}\text{Sn}$ . In case the neck formation dominates the DE process, this is surprising, since the neck region should exhibit a strengthened neutron excess, quite sensitive to the isospin of the target nucleus [4]. In an attempt to select phase-space regions that favor DE emission, we now look at: *i*)  $pp$  correlations in the forward ( $30^\circ \leq \theta \leq 42^\circ$ ) region and *ii*)  $np$  correlations which include very low energy neutrons ( $E_n \geq 2$  MeV, in the lab system). Neutrons with 2–8 MeV energy, detected at  $54^\circ \leq \theta \leq 120^\circ$ , correspond to 15–45 MeV energy in an IS ( $v=0.18c$ ) source.

The results for  $pp$  and  $np$  correlation functions ob-

tained under conditions (*i*) and (*ii*), are shown in Fig. 3. A stronger  $pp$  correlation function is now observed for the more neutron-rich system,  $^{36}\text{Ar}+^{124}\text{Sn}$ . This is true for integrated (a) as well as low- $P_{tot}$  gated (c) correlations. The low- $P_{tot}$  gated correlations show the largest isospin signal. The reason for the relatively large value of the  $P_{tot}$  cut (450 MeV/c), is the necessity to populate the large  $q$  (normalizing) region in the forward ( $30^\circ \leq \theta \leq 42^\circ$ ) detectors. This cut corresponds to TLS protons with  $E_p < 30$  MeV, and IS protons with  $E_p < 20$  MeV. It is these low energy protons that show the largest isospin effect.

The  $np$  correlation functions at angles  $54^\circ$ – $120^\circ$  (Figs. 3b,d,f), show large isospin effects when low energy neutrons,  $2 \leq E_n \leq 8$  MeV, are included (compare with Figs. 2b,d,f). Again, the correlation is stronger for the more neutron-rich system, indicating that the space-time extent of the emitting source is smaller in  $^{124}\text{Sn}$ . In particular, both low- $P_{tot}$  gated (here  $P_{tot} < 240$  MeV/c) correlation functions (Fig. 3d) are enhanced as compared to Fig. 3b (instead of being suppressed as expected for an evaporative source). A plausible explanation for this is that the pairs selected by this gate are dominated by DE particles. Since this effect did not occur in the data where the low energy neutrons were removed (Fig. 2d), we attribute the correlation enhancement to DE particles in the energy range 15–45 MeV, which are favored in the neutron-rich system. If this isospin effect mainly comes from the intermediate energy particles, it should be connected to the density dependence of the nuclear symmetry energy [15,16].

Within the multi-source reaction mechanism described above, composite particles, like deuterons and tritons, are believed to be predominantly emitted from the DE source [30,31], where they are formed by a coalescence mechanism [32]. Let us first remark that neither integrated nor  $P_{tot}$  gated  $dd$ ,  $tt$  and  $dt$  correlation functions show any appreciable difference between the two Sn-targets [33]. This is in agreement with the small sensitivity shown by the calculations of Ref. [34]. Even so, a variation of the correlation functions such as  $nd$ ,  $nt$ , etc. may be expected, as a consequence of the isospin effects on neutrons and protons. Indeed, this is the case in our experimental data, which can be taken as a further evidence for the presence of true isospin effects. Figs. 4a,b present the angle-integrated ( $54^\circ \leq \theta \leq 120^\circ$ )  $nd$  (a) and  $nt$  (b) correlation functions, measured for the two Sn-targets, with a neutron energy threshold of 2 MeV. The anticorrelation observed for  $nd$  pairs (Fig. 4a), has been observed earlier for smaller collision systems, both at lower energies [35] and for 61 A MeV [19]. It may originate from the depletion of low relative momentum  $nd$  pairs due to triton formation [36]. In Fig. 4a the difference in correlation strength between the two Sn-targets can be observed.

The correlation functions of  $nt$  pairs (Fig. 4b), exhibit a broad peak which contains the contributions from the particle-unbound ground state of  $^4\text{H}$ , and possibly from higher lying excited states [37]. Once again, a small enhancement in the strength is observed for the  $^{124}\text{Sn}$ -

target.

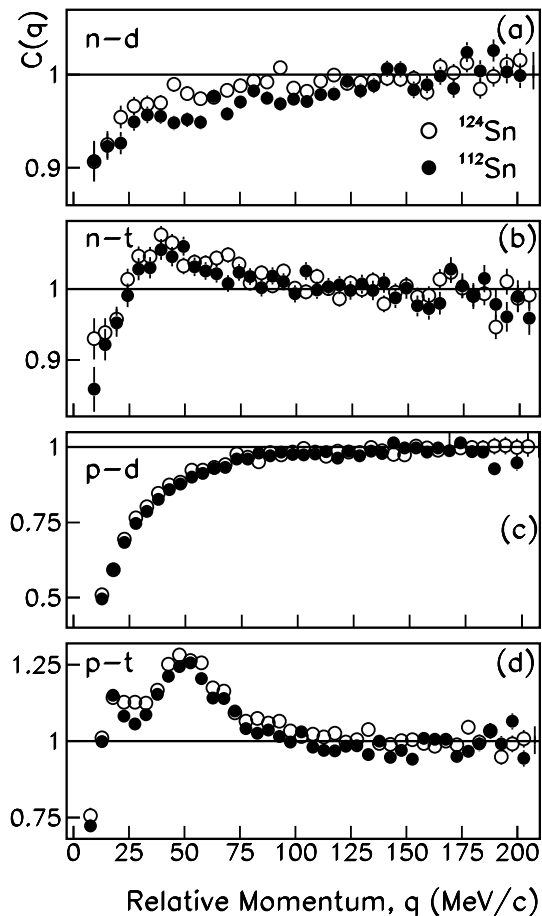


FIG. 4. From  $^{36}\text{Ar}+^{112}\text{Sn}$  (filled symbols) and  $^{36}\text{Ar}+^{124}\text{Sn}$  (open symbols): (a,b)  $nd$ ,  $nt$  ( $54^\circ \leq \theta \leq 120^\circ$ ); (c,d)  $pd$ ,  $pt$  ( $30^\circ \leq \theta \leq 42^\circ$ ).

The  $pd$  and  $pt$  correlation functions, measured in the forward angular range ( $30^\circ \leq \theta \leq 42^\circ$ ), are shown in Figs. 4c,d. The  $pd$  correlation function (c) is characterized by a pronounced anticorrelation at small  $q$ , due to final state Coulomb repulsion. The isospin effect is negligible. The  $pt$  correlation function (d), contains resonance contributions from several excited states of  $^4\text{He}$  [37]. A small isospin effect is seen in this correlation function.

In summary, isospin effects have been investigated in the  $E/A = 61$  MeV  $^{36}\text{Ar}+^{112}\text{Sn}$ ,  $^{124}\text{Sn}$  reactions, and, for the first time, correlation functions from systems similar in size but with different isospin have been experimentally determined. Both angle-integrated and total-momentum gated correlation functions for all different pairs of particles containing  $n$ ,  $p$ ,  $d$  and  $t$ , have been measured. The largest effects from the isospin of the emitting system are seen in the  $np$  correlation function. In particular, gated  $np$  correlation functions which should favor a dynamical emission source, show a stronger correlation for  $^{124}\text{Sn}$  than  $^{112}\text{Sn}$ . This could be explained by different time distributions, with a shorter average emission time

for the neutron-rich system. Smaller isospin effects are also seen in  $pp$ ,  $pt$ ,  $nd$  and  $nt$  correlation functions. These experimental results demonstrate that two-particle correlation functions indeed provide an additional observable to probe the isospin dependence of the nuclear EOS.

The authors wish to thank S. Brandenburg and the AGOR crew, F. Hanappe and the DEMON Collaboration. This work was partly supported by the European Commission (Transnational Access Program, contract HPRI-CT-1999-00109), and by the Swedish Research Council (grant nr F 620-149-2001).

- 
- [1] *Isospin Physics in Heavy-Ion Collisions at Intermediate Energies*, edited by Bao-An Li and W.U. Schröder (Nova Science Publishers, Inc., New York, 2001).
  - [2] P. Danielewicz *et al.*, *Science* **298**, 1592 (2002).
  - [3] H. Müller and B. Serot, *Phys. Rev. C* **52**, 2072 (1995).
  - [4] M. Colonna *et al.*, *Phys. Rev. C* **57**, 1410 (1998).
  - [5] Bao-An Li, *Phys. Rev. Lett.* **85**, 4221 (2000).
  - [6] Y.G. Ma *et al.*, *Phys. Rev. C* **60**, 024607 (1999).
  - [7] J.-Y. Liu *et al.*, *Phys. Rev. C* **63**, 054612 (2001).
  - [8] Bao-An Li *et al.*, *Phys. Rev. Lett.* **78**, 1644 (1997).
  - [9] V. Baran *et al.*, *Nucl. Phys.* **A703**, 603 (2002).
  - [10] Bao-An Li and C.M. Ko, *Nucl. Phys.* **A618**, 498 (1997).
  - [11] H.S. Xu *et al.* *Phys. Rev. Lett.* **85**, 716 (2000).
  - [12] W.P. Tan *et al.*, *Phys. Rev. C* **64**, 051901(R) (2001).
  - [13] M.B. Tsang *et al.*, *Phys. Rev. Lett.* **86**, 5023 (2001).
  - [14] Bao-An Li *et al.*, *Phys. Rev. C* **64**, 054604 (2001).
  - [15] L.W. Chen *et al.*, *Phys. Rev. Lett.* **90**, 162701 (2003).
  - [16] L.W. Chen *et al.*, *Phys. Rev. C* **68**, 014605 (2003).
  - [17] R. Ghetti *et al.*, *Nucl. Inst. Meth.* **A**, in press.
  - [18] R. Ghetti *et al.*, *Nucl. Phys.* **A674**, 277 (2000).
  - [19] R. Ghetti *et al.*, *Phys. Rev. Lett.* **91**, 092701 (2003).
  - [20] V. Avdeichikov *et al.*, *Nucl. Inst. Meth.* **A501**, 505 (2003).
  - [21] C.P. Montoya, *et al.*, *Phys. Rev. Lett.* **73**, 3070 (1994).
  - [22] J. Töke *et al.*, *Phys. Rev. Lett.* **75**, 2920 (1995).
  - [23] Y. Larochelle *et al.*, *Phys. Rev. C* **55**, 1869 (1997).
  - [24] J. Lukasik *et al.*, *Phys. Rev. C* **55**, 1906 (1997).
  - [25] P. Pawloski *et al.*, *Phys. Rev. C* **57**, 1771 (1998).
  - [26] Y. Larochelle *et al.*, *Phys. Rev. C* **59**, R565 (1999).
  - [27] E. Plagnol *et al.*, *Phys. Rev. C* **61**, 014606 (1999).
  - [28] P.M. Milazzo *et al.*, *Nucl. Phys.* **A 703**, 466 (2002).
  - [29] J. Lukasik *et al.*, *Phys. Lett. B*, **566**, 76 (2003).
  - [30] G. Lanzanò *et al.*, *Nucl. Phys.* **A 683**, 566 (2001).
  - [31] T. Lefort *et al.*, *Nucl. Phys.* **A 662**, 397 (2000).
  - [32] W.J. Llope *et al.*, *Phys. Rev. C* **52**, 2004 (1995).
  - [33] R. Ghetti *et al.*, to be published.
  - [34] L.W. Chen, C.M. Ko, Bao-An Li, arXiv:nucl-th/0306032, 2003.
  - [35] R.A. Kryger *et al.*, *Phys. Rev. Lett.* **65**, 2118 (1990).
  - [36] L. Tomio *et al.*, *Phys. Rev. C* **35**, 441 (1987).
  - [37] D.R. Tilley *et al.*, *Nucl. Phys.* **A 541**, 1 (1992).